ORIGINAL RESEARCH

# Synthesis, characterization, and in vivo efficacy evaluation of PGG–docetaxel conjugate for potential cancer chemotherapy

Danbo Yang[1]
Sang Van[2]
Yingyi Shu[1]
Xiaoqing Liu[1]
Yangfeng Ge[1]
Xinguo Jiang[3]
Yi Jin[2]
Lei Yu[1,2]

[1]Biomedical Engineering and Technology Institute, Institutes for Advanced Interdisciplinary Research, East China Normal University, Shanghai, People's Republic of China; [2]Biomedical Group, Nitto Denko Technical Corporation, CA, USA; [3]School of Pharmacy, Fudan University, Shanghai, People's Republic of China

**Aim:** This work is intended to develop and evaluate a biopolymeric poly(L-γ-glutamyl-glutamine) (PGG)–docetaxel (DTX) conjugate that can spontaneously self-assemble in aqueous solutions to become nanoparticles.

**Methods:** DTX was covalently attached to hydrophilic PGG by direct esterification, and the conjugate was characterized by proton nuclear magnetic resonance spectroscopy, molecular weight gel permeation chromatography, solubility, size distribution and morphology, and hemolysis. Conjugated DTX was found to have 2000 times improved water solubility compared with free DTX. Dynamic light scattering, transmission electron microscopy, and atomic force microscopy revealed the particle size, distribution and morphology of the PGG–DTX conjugate. In addition, the conjugate was further tested for in vitro cytotoxicity and in vivo antitumor efficacy on the human non-small cell lung cancer cell line NCI-H460.

**Results:** Conjugated DTX was found to have 2000 times improved water solubility compared with free DTX. The conjugate formed nanoparticles with an average diameter of 30 nm in spherical shape and unimodal particle size distribution. The conjugate exhibited about 2% hemolysis at 10 mg/mL, compared with 56% for Tween 80® at 0.4 mg/mL, and 33% for Cremophor EL® at 10 mg/mL. In addition, the conjugate was further tested for in vitro cytotoxicity and in vivo antitumor efficacy on the human non-small cell lung cancer cell line NCI-H460. As expected, conjugated DTX exhibited lower cytotoxicity compared to that of free DTX, in concentration-dependent manner. However, PGG–DTX showed better antitumor activity in NCI-H460 lung cancer-bearing mice with minimal weight loss compared to that of free DTX.

**Conclusion:** The PGG–DTX conjugate may be considered as an attractive and promising polymeric DTX conjugate for non-small cell lung cancer treatment.

**Keywords:** polymer drug delivery, nanotechnology, nanotherapeutics, drug delivery, nanomedicine, pharmaceutics

## Introduction

Docetaxel (DTX) is a hydrophobic semisynthetic analog of paclitaxel.[1] DTX is approved by the US Food and Drug Administration (FDA) to be used alone or with other drugs as second-line treatment for patients with advanced/metastatic non-small cell lung cancer.[2] It is also approved by the FDA for use in combination with cisplatin and 5-fluorouracil for the induction treatment of patients with locally advanced squamous cell carcinoma of the head and neck and for the treatment of patients with advanced gastric adenocarcinoma. In 2004, the FDA approved DTX for use in combination with doxorubicin and cyclophosphamide for the adjuvant treatment of women with operable node-positive breast cancer, and for use in combination with prednisone for the treatment of metastatic, androgen-independent (hormone-refractory) prostate cancer.[3] In terms of toxicity, the main grade 3–4 toxicity of the current clinical DTX formulation, which

Correspondence: Lei Yu
Nitto Denko Technical Corporation,
501 Via Del Monte, Oceanside,
CA 92028, USA
Tel +1 760 435 7026
Fax +1 760 435 7050
Email yu_lei@gg.nitto.co.jp

**581**

features nonionic surfactant Tween 80® and ethanol (50:50, v/v) as the excipients, were neutropenia and leukopenia.[2,4–8] Currently, a number of strategies are being employed to develop novel, surfactant (Tween 80)-free formulations of DTX.[9] These formulations include lecithin-in-water emulsions of DTX,[10] DTX–liposomes,[11,12] DTX-loaded glycol chitosan nanoparticles,[13] DTX-loaded micelles,[14–16] DTX-loaded solid lipid nanoparticles,[17] and DTX-loaded poly(lactic acid)-poly(ethylene glycol) nanoparticles.[18] In addition to the abovementioned approaches, DTX conjugation is another strategy to eliminate the side effects of Tween 80 and ethanol. Some examples of DTX conjugates include luteinizing hormone-releasing hormone receptor peptide,[19] linoleic,[20] methoxy polyethylene glycol,[16] albumin protein,[21] low molecular weight chitosan,[22] and N-(2-hydroxypropyl)-methacrylamide copolymers.[23] Similar to the non-conjugated formulations of DTX discussed above, the development of these DTX conjugates is also in the early stages. Only limited polymers are suitable as drug delivery vehicles because of the requirement for biocompatibility and biodegradability.[24]

Very recently, we reported the synthesis, pharmacokinetics, and efficacy of poly(L-g-glutamylglutamine-paclitaxel) conjugate (PGG-paclitaxel conjugate).[25–27] The effectiveness of the PGG–paclitaxel (PTX) conjugate for treating cancer is likely to be a result of various factors including: (1) the increased water solubility of paclitaxel by conjugation to water-soluble polymer PGG, which could avoid the use of surfactants or excipients, and the PGG–PTX conjugate can be dissolved in saline or phosphate-buffered saline (PBS) for intravenous injection; (2) "enhanced permeability and retention" effects that were related to the preferential accumulation of PGG–PTX conjugate in hypervascular tumor tissue and low excretion from kidney filtration due to the high molecular weight of the conjugate; (3) self-assembling of PGG–PTX conjugate into nanoparticles of less than 50 nm, which might contribute to passive tumor targeting; (4) increased tumor accumulation of active paclitaxel might be due to the selective release of paclitaxel mediated by high local tumor carboxylesterases and/or tumor macrophages; (5) improved therapeutic index by exposure to the slow, prolonged release of paclitaxel from the conjugate. Encouraged with the results, we hypothesized that the PGG–drug conjugate could be used as a technological platform capable of improving the efficacy of anticancer drugs. However, since the physicochemical properties of each PGG–drug conjugate may be different, we are currently exploring one drug at a time with the platform of PGG-drug conjugate. Herein we report the synthesis, physical properties, hematological toxicity, in vitro cytotoxicity, and in vivo antitumor efficacy of the PGG–DTX conjugate.

# Materials and methods
## Materials
Poly(L-glutamic acid), sodium salt (Mw 20 kDa), dimethylformamide, sodium bicarbonate, and 4-di(methylamino) pyridine were purchased from Sigma-Aldrich Chemical Co, (St Louis, MO). N-(3-dimethylaminopropyl)-N′-ethylcarbodiimide, L-glutamic acid di-*tert*-butyl ester hydrochloride, and trifluoroacetic acid were purchased from Novabiochem (La Jolla, CA). 1-Hydroxybenzotriazole was purchased from Spectrum (Gardena, CA). DTX was purchased from NuBlocks (Vista, CA). All the chemicals and reagents were used as received without further purification.

## Mice and cell lines
Female BALB/c nude mice, 6–8 weeks of age, were from Vital River Laboratories, Inc (Beijing, China). The NCI-H460 cell line was obtained from the American Type Culture Collection (Manassas, VA) and grown in RPMI 1640 medium (Sigma-Aldrich) supplemented with 10% fetal bovine serum, 100 U/mL of penicillin (Invitrogen, Carlsbad, CA), and 100 µg/mL of streptomycin (Invitrogen).

## Synthesis of PGG–DTX conjugate
Synthesis of the PGG–DTX conjugate was carried out following our previously published procedure[25] with the modification of replacing paclitaxel with DTX. Briefly, PGG–DTX was synthesized in a two-step process. First, PGG was prepared from poly(L-glutamic acid), sodium salt, Mw 20 kDa) with the addition of L-glutamic acid di-*tert*-butyl ester hydrochloride in the presence of 1-hydroxybenzotriazole and N-(3-dimethylaminopropyl)-N′-ethylcarbodiimide in anhydrous dimethylformamide solvent. Subsequently, the t-butyl ester protecting group from PGG–di-*tert*-butyl ester intermediate was deprotected with trifluoroacetic acid under anhydrous conditions, and PGG was isolated after dialysis against water and lyophilization. Subsequently, PGG–DTX was synthesized by coupling DTX with PGG in the presence of N-(3-dimethylaminopropyl)-N′-ethylcarbodiimide coupling agent and a trace of 4-di(methylamino) pyridine catalyst in anhydrous dimethylformamide solvent. The reaction mixture was stirred continuously for 24 hours at room temperature. The reaction was determined as completed by thin layer chromatography (spot of the DTX disappeared in ethyl acetate). Then, the solution was poured into an excess amount of 0.2 M HCl, and the precipitate was collected. PGG–DTX was re-dissolved in 0.3 M $NaHCO_3$ and dialyzed against water overnight (15 hours). Finally, the PGG–DTX conjugate was obtained after lyophilization.

## Characterization

### ^{1}H-NMR spectroscopy and gel permeation chromatography measurement

^{1}H-NMR spectra were obtained on an NMR spectrometer (Varian, Palo Alto, CA) using $CDCl_3$ for DTX and $D_2O$ for PGG–DTX. Chemical shifts were reported in ppm. Gel permeation chromatography measurements were performed using a gel permeation chromatography–multi-angle light-scattering detector. This was operated with a ChemStation program with Agilent 1200 analytical series and ASTRA V program with Wyatt Technology Company Dawn Heleos light-scattering detector and refractive index detector. The column was Shodex OHpak, SB 804HQ (Phenomenex, Torrance, CA) with a guard column, SB-G 605038. The mobile phase was phosphate buffer solution (50 mM phosphate, 50 mM sodium chloride, 200 ppm sodium azide, pH 6.5) and 45% $CH_3OH$ (high-performance liquid chromatography grade) by volume to volume. The injection volume was 100 μL and the elution was isocratic at a flow rate of 0.7 mL/minute over 30 minutes with additional ultraviolet detection at 228 nm.

### Determination of DTX content and solubility of the PGG–DTX conjugate

The conjugate was dissolved in distilled water, and its ultraviolet–visible absorbance at 228 nm was measured.[22] DTX content of the conjugate was determined based on a standard curve generated with a known concentration of DTX in methanol solution. The solubility of the conjugate was measured by gravimetric analysis. A saturated solution of PGG–DTX was prepared with excess conjugate. The solutions were stirred for 5 hours at room temperature and then filtered through a 0.45 μm PTFE syringe filter and lyophilized (FreeZone Benchtop and Console Freeze Dry System, Labconco, Kansas City, MO). After 48 hours, the dry powder was weighed and solubility was calculated as mg/mL.

### Dynamic light-scattering (DLS) measurements

The particle size of the polymer conjugate solution was determined by DLS using a ZETASIZER Nano-ZS (Malvern Instruments Inc, UK) equipped with He–Ne laser (4 mW, 633 nm) light source and 90° angle scattered-light collection configuration. Polymer conjugate solution (2.0 mg/mL) was prepared in saline and the samples were equilibrated for 5 minutes at 25°C before the measurements. Each sample was measured with 10 runs and 10 seconds duration before each run, and measurements were repeated three times. All the measurements were done in triplicate, and average particle sizes were presented as the average diameter with standard deviation.

### Transmission electron microscopy (TEM) and atomic force microscopy (AFM)

The morphology of PGG–DTX nanoparticles was observed using two techniques, (1) TEM and (2) AFM, to visualize the interface of the polymer at nanoscale. The TEM study was carried out using a TEM H-7000 (Hitachi, Tokyo, Japan) electron microscope operating at an accelerating voltage of 75 kV. Negative staining was performed as follows: (1) a drop of sample solution was placed onto a copper grid coated with carbon, (2) the sample drop was tapped with a filter paper to remove surface water and air-dried for 5 minutes followed by the application of 0.01% phosphotungstic acid to deposit the micelles on the grid, and (3) the samples were air-dried before observation. The AFM studies were performed using a NanoScope III a MultiMode AFM (Digital Instruments/ Veeco Metrology Group, Santa Barbara, CA). One drop of the nanoparticle dispersion (0.05 mg/mL) was placed on the surface of fresh cover slip and air-dried at room temperature. The AFM measurements were operated in tapping mode.

## Hemolysis of the PGG–DTX nanoparticles

Hemolysis study was carried out according to the published procedure.[28] Briefly, freshly collected rat blood was washed three times with PBS solution (pH 7.4) by centrifugation at 1000 rpm for 5 minutes. The red blood cell suspension was diluted with saline to obtain a 2% suspension (v/v). Various concentrations of PGG-DTX, Tween 80 (Wei'er Chem, Nanjing, China), Cremophor EL® (Sigma-Aldrich), and saline samples in phosphate buffer were added into the RBC suspension. After incubation at 37°C for 1 hour, samples were centrifuged at 3000 rpm for 10 minutes to remove non-lysed RBC. The supernatants were collected and analyzed for hemoglobin content by spectrophotometric detection at 416 nm. Analysis of each sample was performed in triplicate. The data are presented as the mean with the standard deviation of the triplicate experiments after they were normalized with the data of the saline hemolysis. The results of the PGG–DTX hemolysis were compared with those of Tween 80 and Cremophor EL.

## In vitro cytotoxicity assay

The cytotoxicity of PGG–DTX nanoparticles and free DTX against the human non-small cell lung cancer NCI-H460 cell line was evaluated using the (3-(4,5-dimethylthiazol-2-yl)-5-(3-carboxymethoxyphenyl)-2-(4-sulfophenyl)-2H-tetrazolium) (MTS) method.[25] Briefly, 100 μL of cell suspension in culture medium at a concentration of $3 \times 10^4$ cells/mL was seeded in each well of a 96-well plate, and incubated at 37°C in a humidi-

fied atmosphere with 5% $CO_2$. After overnight incubation, serial dilutions of PGG–DTX were added to the plate (100 μL/well). After further incubation for up to 72 hours, the cells were stained with MTS reagent (Promega). The absorbance at 490 nm was measured with a microplate reader (Thermo Multiskan MK3; Thermo Scientific, Waltham, MA). Survival was calculated as the absorbance in wells of treated cells and normalized to controls, and the concentration of drug that inhibited cell survival by 50% ($IC_{50}$) was calculated by GraphPad Prism (v 5; GraphPad Software, Inc, San Diego, CA).

## Evaluation of antitumor activity in human tumor xenograft models

Tumor fragments ($3 \times 3 \times 3$ mm) of H460 cell were implanted subcutaneously in 6–8 week-old female nu/nu nude mice (Vital River, Beijing, China). Tumor diameters were measured two or three times per week using a sliding caliper. The tumor volume (TV) was calculated according to the formula TV = $(L \times W^2)/2$, where L and W were the length of the major and minor diameters, respectively. The drug treatment was started when the tumors reached a size of 100 mm³. The tumor-bearing mice were randomly divided into six groups, with six mice to each group (n = 6). PGG–DTX was administered intravenously via tail-vein injection at doses of 20 mg/kg, 40 mg/kg, 60 mg/kg, and 80 mg/kg, to four separate groups of tumor-bearing mice three times within a 3-day interval. DTX at the maximum tolerated dose of 5 mg/kg and PBS solution were administered using the same injection method to one positive control group and one negative control group, respectively, of tumor-bearing mice.

## Statistical analysis

The statistical significance of the data was evaluated by student's $t$ test, and $P < 0.05$ was considered significant.

## Results and discussion

The rationale of utilizing a macromolecular polymer–drug conjugate to improve the therapeutic indices of a small molecular anticancer drug is based on the concept of the combined effects of "enhanced permeability and retention." These effects are attributed to disrupted vasculature, insufficient lymphatic drainage in the tumor tissue, and prolonged circulation time of a polymer-conjugated anticancer drug. By avoiding kidney filtration, such conjugates can passively accumulate in the targeted tumors.[29,30] Recently, a number of polymer–anticancer drug conjugates were tested in clinical trials.[31] The polymers included N-(2-hydroxypropyl)methacrylamide, poly(L-glutamate), and poly(ethylene glycol); the drugs conjugated were doxorubicin,

paclitaxel, palatinate, and camptothecin. The poly(L-glutamic acid)–paclitaxel conjugate (CT-2103) is considered the most advanced polymer–paclitaxel conjugate to date[32] and has been investigated in multiple Phase III clinical trials. However, CT-2103 is not yet approved by the FDA for cancer treatment.[33–35]

## ¹H-NMR spectra, molecular weight, and solubility of polymers

DTX was covalently attached to PGG through a direct esterification that is known to be hydrolyzed under physiological conditions. Conjugation between PGG and DTX was carried out using a similar procedure to that previously described by our laboratory for the synthesis of the PGG–paclitaxel conjugate.[25] The conjugate was characterized by ¹H-NMR, showing corresponding peaks to both PGG and DTX conjugated (Figure 1B and 1D, respectively). DTX free and conjugated were identified and confirmed by proton chemical shifts at 7.0–8.0 ppm for its aromatic protons (Figure 1C and 1D, respectively). The resonance at 4.0–4.5 ppm was assigned to the methylene protons of the PGG backbone (Figure 1B and D).

The molecular weights of the obtained polymers, as well as the polydispersity indices, were calculated by gel permeation chromatography with multi-angle light-scattering detection. The average molecular weight of PGG and PGG–DTX was about 40 kDa and 90 kDa, respectively, with low polydispersity index (Table 1). The weight percentage of DTX in the PGG–DTX conjugate was determined to be ~38 weight percent by measuring ultraviolet absorption at a wavelength of 228 nm.[25] The solubility of the PGG–DTX conjugate was >15 mg/mL of DTX equivalent, compared to that of free DTX which was reported to be approximately 6–7 μg/mL. Thus, the increase in solubility of conjugated DTX was approximately 2000-fold. This improved water solubility enabled the PGG–DTX conjugate to be dissolved in saline or PBS for in vitro and in vivo experiments without using Tween 80, ethanol, or other surfactants.

## DLS and TEM morphology

The nanoparticle size and size distribution were measured by DLS. As depicted in Figure 2, the mean size of PGG–DTX nanoparticle dispersion was about 30 nm. The conjugate exhibited unimodal particle size distribution with a low polydispersity index of 0.225, which indicated that the dispersion was homogeneous. The average particle size and distribution of the PGG–DTX conjugate were confirmed by TEM and AFM that were used to directly visualize the size and morphology of the PGG–DTX conjugate in the dry state (Figures 2 and 3), showing the nanoparticles were spherical with diameters around 20–30 nm. The particle size of the PGG–DTX conjugate was
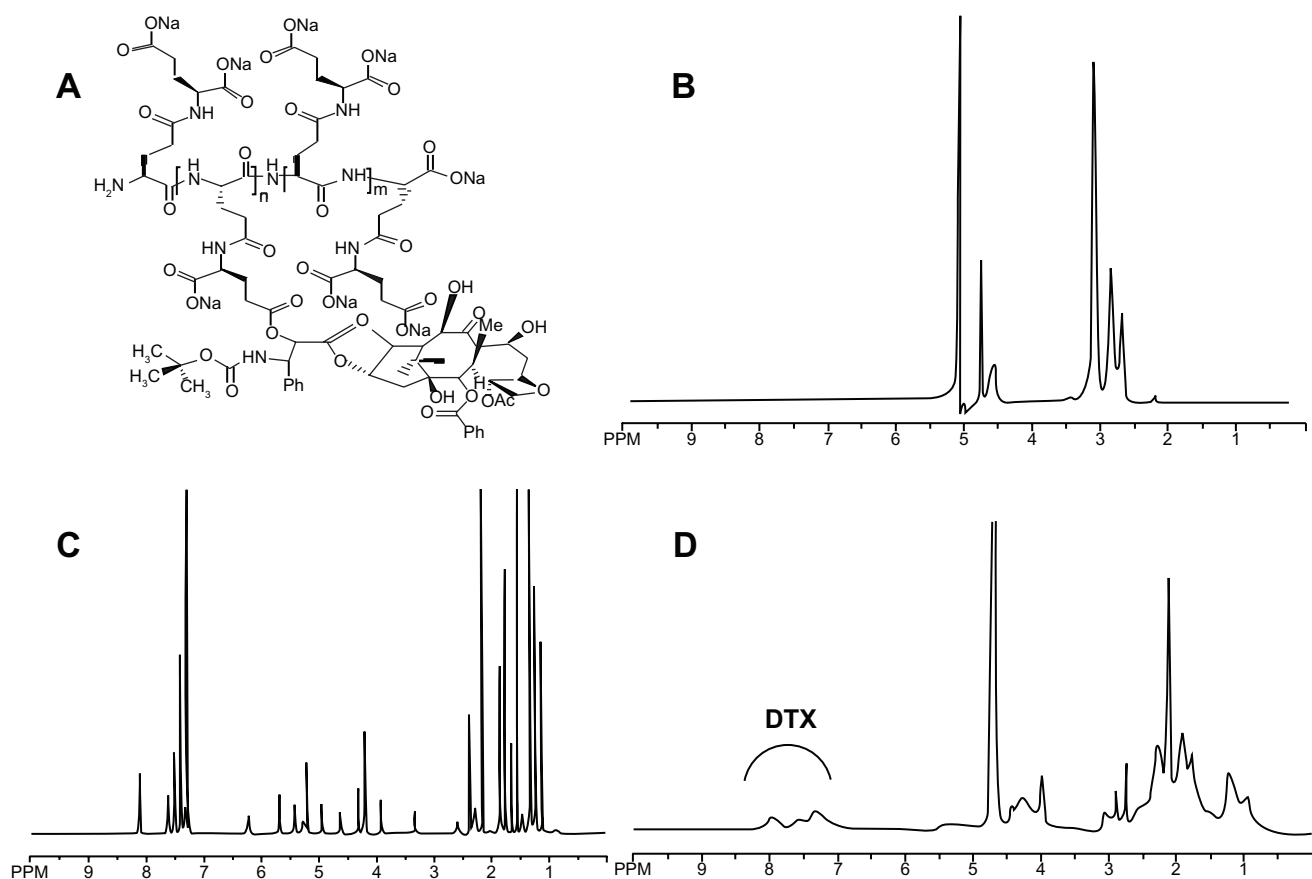
**Figure 1** (**A**) The chemical structure of the PGG–DTX conjugate. ¹H-NMR spectra of PGG polymer-length chain (**B**), free docetaxel (**C**) in CDCl₃ in D₂O and PGG–DTX nanoparticles (**D**).
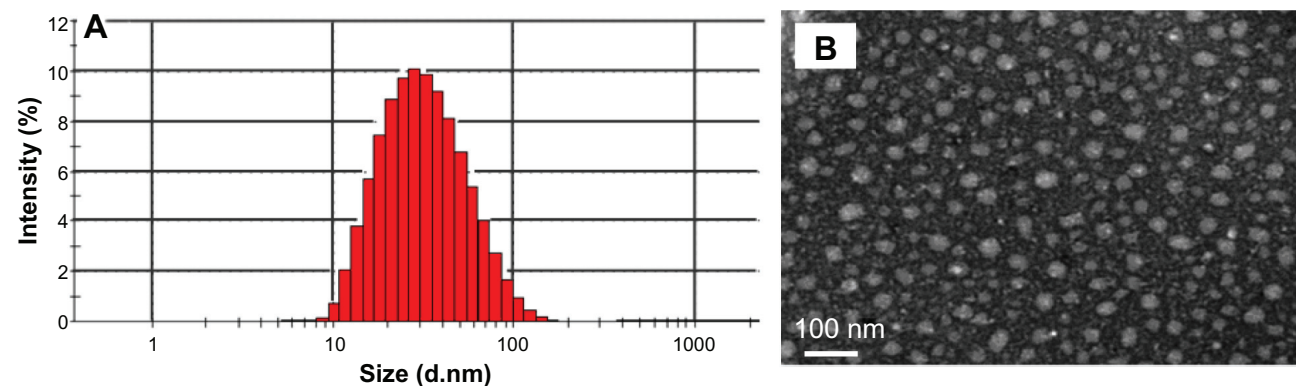**Abbreviations:** PGG, poly(L-γ-glutamyl-glutamine); DTX, docetaxel.



**Figure 2** Characterization of the PGG–DTX nanoparticles. The particle size and polydispersity of the PGG–DTX conjugate obtained from (**A**) dynamic light scattering, and (**B**) transmission electron microscopy.
**Abbreviations:** PGG, poly(L-γ-glutamyl-glutamine); DTX, docetaxel; Mw, weight average molecular weight; Mn, number average molecular weight.

**Table 1** Physical characteristics of the PGG–DTX conjugate

| Conjugate | DTX feeding ratio (%) | DTX content (%) | Zeta potential | Size (nm) | Polydispersity | Molecular weight | | |
| --- | --- | --- | --- | --- | --- | --- | --- | --- |
| | | | | | | Mw | Mn | Mw/Mn |
| PGG | N/A | N/A | N/A | N/A | N/A | 39.5 | 33.2 | 1.19 |
| PGG–DTX | 35% | 38.2 | −21.3 | 28.3 | 0.225 | 89.3 | 59.7 | 1.50 |

**Abbreviations:** PGG, poly(L-γ-glutamyl-glutamine); DTX, docetaxel; Mw, weight average molecular weight; Mn, number average molecular weight.

**Dovepress**
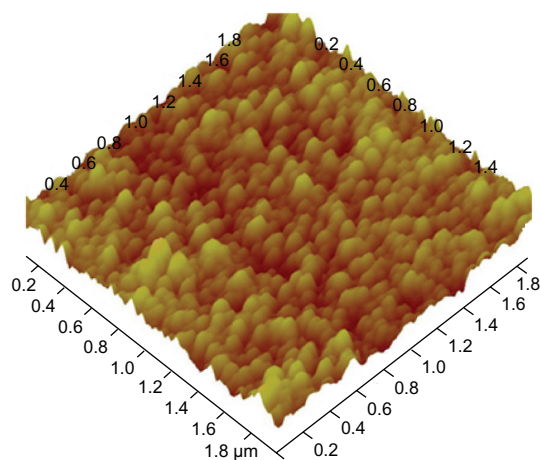
**Figure 3** Tapping mode atomic force microscopy image of the poly(L-γ-glutamyl-glutamine)–docetaxel conjugate.



**Figure 4** Hemolysis of red blood cells after incubation with PGG–DTX, Tween 80®, and Cremophor EL®.
**Note:** Data reported as means of three independent experiments ± standard error.
**Abbreviations:** PGG, poly(L-γ-glutamyl-glutamine); DTX, docetaxel.

consistent with the particle size of the PGG–paclitaxel conjugate, which was previously reported.[36,37] Zeta potential or particle surface charge is an important parameter, indicating the stability of nanocarrier systems. A relatively high surface charge may provide a repelling force between the particles, thus they could be more stable in solution due to less aggregation.[38] Table 1 shows that the PGG–DTX conjugate had high negative zeta potentials of –21.3 mV due to the presence of two ionized carboxylic acid groups in the PGG polymer backbone. It is reasonable to conclude that the charged particles may repel each other and prevent aggregation or precipitation.

## Hemolysis

To determine whether PGG–DTX induces membrane damage, a hemolysis study was conducted using procedures described in the literature.[28] Our previous study showed that the backbone PGG carrier inherited good biocompatibility.[25] In this study, PGG-DTX showed no hemolytic activity even at high concentrations of 10 mg/mL compared with those of the surfactant Tween 80, which caused significant red blood cell damage at low concentrations of 0.2–0.5 mg/mL to 1.0–2.0 mg/mL (Figure 4). Cremophor EL did not induce substantial hemolysis until reaching its concentration of 4 mg/mL. Significantly, hemolytic activity of PGG–DTX was almost negligible even at high concentrations of 10 mg/mL. The results suggested that PGG–DTX would not induce anemic toxicity following systemic intravenous uses.

## Cytotoxicity

The cytotoxicity of PGG–DTX was evaluated by the MTS method using NCI-H460 as the model human non-small lung cancer cell line, with formulated DTX as the control in Tween 80:ethanol (1:1, v/v). As shown in Figure 5, the backbone
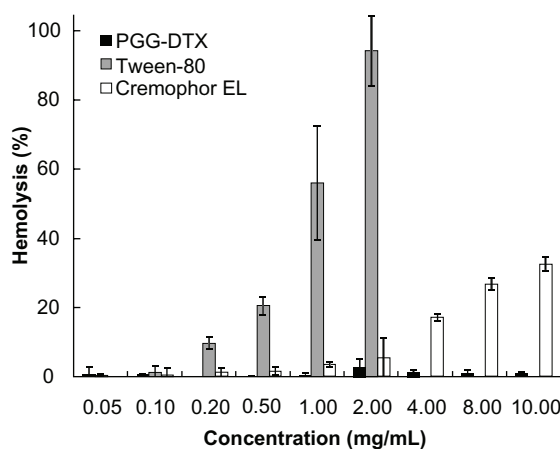
carrier PGG did not cause significant cytotoxicity against the NCI-H460 cell line at experimental concentrations up to 0.50 mg/mL. However, PGG–DTX and DTX were cytotoxic in a concentration-dependent manner. Experimental $IC_{50}$ values of PGG–DTX and DTX were found to be $88.1 \pm 23.7$ and $4.1 \pm 0.3$ μg/L, respectively. As expected, the $IC_{50}$ value of PGG–PTX was higher than the $IC_{50}$ value of DTX, which indicated that DTX was still in a conjugated form and partially released into a free DTX form. At PGG–DTX concentrations of 0.01 mg/mL, the cell viability was reduced to 20%, while treatment with formulated free DTX reached this maximum cytotoxicity at a concentration of 0.0001 mg/mL (Figure 5).
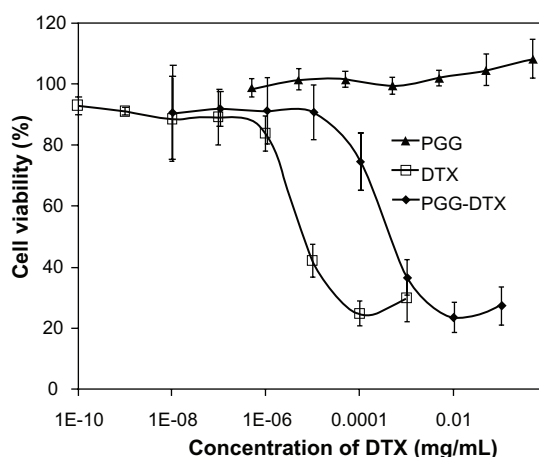


**Figure 5** In vitro cytotoxicity study of cells treated with free DTX or PGG–DTX for 72 hours at 37°C, evaluated by (3-(4,5-dimethylthiazol-2-yl)-5-(3-carboxymethoxyphenyl)-2-(4-sulfophenyl)-2H-tetrazolium) (MTS) assay, and expressed as percentage of untreated cells.
**Note:** Data reported as means of three independent experiments ± standard error.
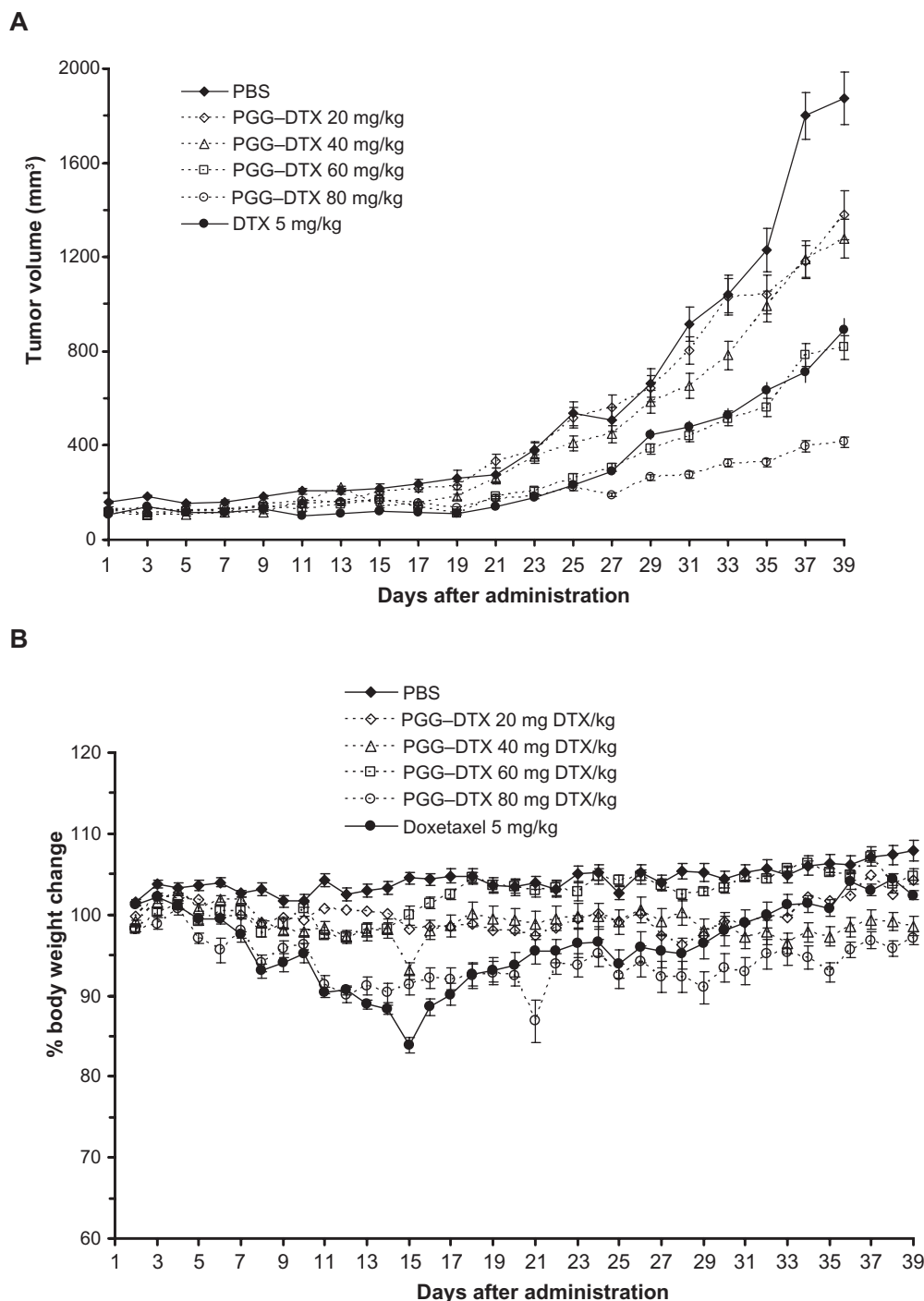**Abbreviations:** PGG, poly(L-γ-glutamyl-glutamine); DTX, docetaxel.

**Figure 6** Antitumor efficacy in nude mice bearing NCI-H460 human non-small cell lung carcinoma tumors. (**A**) Mean tumor growth curves. (**B**) Body weight change.
**Note:** Data presented as means ± standard error.
**Abbreviations:** PBS, phosphate-buffered saline; PGG, poly(L-γ-glutamyl-glutamine); DTX, docetaxel.

## PGG–DTX can be more potent and less toxic than DTX in a lung cancer model

Human non-small cell lung H460 carcinoma xenograft models were prepared to assess the effectiveness of the PGG–DTX conjugate in terms of inhibiting tumors in vivo. To determine the effect of the drugs on H460 tumor growth, PGG–DTX or DTX was given as three repeated intravenous administrations as q3d × 3 after subcutaneous tumor implantation. Antitumor activity was evaluated using the doses equal to or less than the maximum tolerated dose of each of the drugs. Tumor growth and body weight change of each group of mice were monitored and recorded.

**Table 2** Tumor-growth inhibition rates of PGG–DTX and docetaxel against H460 carcinoma cells which were inoculated subcutaneously into nu/nu mice

| Treatment group | Dose (mg/kg/day)[a] | Antitumor activity | | Toxicity | |
| --- | --- | --- | --- | --- | --- |
| | | Mean tumor volume (mm³)[b] day 37 | Tumor inhibition rate[c] day 37 | DRD[d] | Mean body weight day 37 vs day 1 |
| Untreated | – | 1800.4 ± 238.5 | – | 0/6 | 107.2 |
| PGG–DTX | 20 | 1181.0 ± 168.3 | 34.40 | 0/6 | 104.9 |
| PGG–DTX | 40 | 1191.9 ± 157.9[e] | 33.80 | 0/6 | 99.1 |
| PGG–DTX | 60 | 785.5 ± 118.7[e] | 56.37 | 0/6 | 107.0 |
| PGG–DTX | 80 | 396.2 ± 55.0[e,f] | 77.99 | 0/6 | 96.6 |
| Docetaxel | 5 | 711.7 ± 99.7[e] | 60.47 | 0/6 | 103.0 |

**Notes:** PGG–DTX and docetaxel were administered intravenously, with three injections administered in a 3-day interval. Tumor volumes were measured every 2 days and body weights were measured daily. [a]The dose of PGG–DTX is expressed as a dose equivalent to docetaxel; [b]each value represents the mean ± standard error of six mice; [c]tumor-growth inhibition rate $(1 - T/C) \times 100$, where T and C are the tumor volume of the treated and control groups, respectively; [d]DRDs within 15 days of last dose; [e]significant difference in comparison with the untreated group ($P < 0.05$); [f]significant difference in comparison with the non-polymer-bound docetaxel-treated group ($P < 0.05$).
**Abbreviations:** PGG, poly(L-γ-glutamyl-glutamine); DTX, docetaxel; DRD, drug-related death.

Figure 6 shows a plot of tumor volume and weight loss as a function of time in mice bearing NCI-H460 lung cancer. These mice were treated for 3 days with three doses of either PBS (negative control), PGG–DTX (20 mg/kg, 40 mg/kg, 60 mg/kg, 80 mg/kg), or DTX (5 mg/kg, positive control). The PBS-treated group of mice showed a progressive increase in tumor growth for mean tumor volume up to day 37. The mice treated with DTX (5 mg/kg) showed significant tumor-growth inhibition ($P < 0.05$), relative to the PBS group (Figure 6A). However, DTX treatment caused an obvious decrease in body weight on day 15, which slowly recovered to its normal value (Figure 6B). In contrast, PGG–DTX treatments of 20 mg/kg, 40 mg/kg, 60 mg/kg, and 80 mg/kg DTX equivalent caused minimal weight loss, within an acceptable range of 10%. Tumor-growth inhibition of PGG–PTX treatment (60 mg/kg DTX equivalent) was comparable to that of the treatment of free DTX (5 mg/kg), and inhibition of tumor growth of PGG–DTX treatment (80 mg/kg DTX equivalent) outperformed the treatment of free DTX 5 mg/kg, in a statistically significant manner. Table 2 shows – after treatment with PGG–DTX and DTX – the tumor-growth inhibition rate and tumor volume on day 37, drug-related deaths up to day 37, and mean body weight on day 37 versus day 1, as a mean ± standard error of six mice/group. No drug-related deaths were observed. The tumor volume and tumor-inhibition rate of mice treated with 20 mg/kg and 40 mg/kg DTX equivalent of PGG–DTX on day 37 were the same. However, as the dose of PGG–DTX increased from 40 mg/kg to 60 mg/kg, and to 80 mg/kg of DTX equivalent, the mean tumor volume decreased linearly, while tumor-inhibition rate increased linearly. These results clearly indicate the superiority of PGG–DTX over DTX, demonstrating that the proper use of macromolecular carriers can increase the potency and the therapeutic indices of DTX.

## Conclusion

In this work, biopolymer backbone PGG was successfully employed for the delivery of the hydrophobic anticancer drug DTX. PGG–DTX nanoparticles were achieved with high solubility, small size, uniform distribution, and biocompability. The in vitro studies demonstrated that PGG–DTX was less cytotoxic compared with free DTX in a dose-dependent manner against NCI-H460 cells. The PGG–DTX conjugate showed in vivo antitumor efficacy to DTX at 80 mg/kg, and the toxicity in terms of body weight loss was markedly reduced compared to that of DTX. Taken together, our PGG–DTX conjugate can be considered as an alternative and promising biocompatible polymer to be used as a delivery system for cancer chemotherapy.

## Acknowledgments

## Disclosure

The authors report no conflicts of interest in this work.

## References

1. Heo JH, Park SJ, Kang JH, et al. Development of new efficient synthetic methods for docetaxel. *Bull Korean Chem Soc*. 2009;30:25–26.
2. Pallis AG, Agelaki S, Agelidou A, et al. A randomized phase III study of the docetaxel/carboplatin combination versus docetaxel single-agent as second line treatment for patients with advanced/metastatic non-small cell lung cancer. *BMC Cancer*. 2010;10:633.
3. Tannock IF, de Wit R, Berry WR, et al; TAX 327 Investigators. Docetaxel plus prednisone or mitoxantrone plus prednisone for advanced prostate cancer. *N Engl J Med*. 2004;351:1502–1512.
4. Harvey V, Mouridsen H, Semiglazov V, et al. Phase III trial comparing three doses of docetaxel for second-line treatment of advanced breast cancer. *J Clin Oncol*. 2006;4:4963–4970.

5. Kudoh S, Takeda K, Nakagawa K, et al. Phase III study of docetaxel compared with vinorelbine in elderly patients with advanced non-small-cell lung cancer: results of the West Japan Thoracic Oncology Group Trial (WJTOG 9904). *J Clin Oncol*. 2006;24:3657–3663.

6. Schuette W, Nagel S, Blankenburg T, et al. Phase III study of second-line chemotherapy for advanced non-small-cell lung cancer with weekly compared with 3-weekly docetaxel. *J Clin Oncol*. 2005;23: 8389–8395.

7. Okada S, Sakata Y, Matsuno S, et al. Phase II study of docetaxel in patients with metastatic pancreatic cancer: a Japanese cooperative study. Cooperative Group of Docetaxel for Pancreatic Cancer in Japan. *Br J Cancer*. 1999;80:438–443.

8. Sulkes A, Smyth J, Sessa C, et al. Docetaxel (Taxotere) in advanced gastric cancer: results of a phase II clinical trial. EORTC Early Clinical Trials Group. *Br J Cancer*. 1994;70:380–383.

9. Ten Tije AJ, Verweij J, Loos WJ, Sparreboom A. Pharmacological effects of formulation vehicles : implications for cancer chemotherapy. *Clin Pharmacokinet*. 2003;42:665–685.

10. Yanasarn N, Sloat BR, Cui Z. Nanoparticles engineered from lecithin-in-water emulsions as a potential delivery system for docetaxel. *Int J Pharm*. 2009;379:174–180.

11. Zhai G, Wu J, Yu B, Guo C, Yang X, Lee RJ. A transferrin receptor-targeted liposomal formulation for docetaxel. *Nanosci Nanotechnol*. 2010;10:5129–5136.

12. Immordino ML, Brusa P, Arpicco S, Stella B, Dosio F, Cattel L. Preparation, characterization, cytotoxicity and pharmacokinetics of liposomes containing docetaxel. *J Control Release*. 2003;91:417–429.

13. Hwang HY, Kim IS, Kwon IC, Kim YH. Tumor targetability and antitumor effect of docetaxel-loaded hydrophobically modified glycol chitosan nanoparticles. *J Control Release*. 2008;128:23–31.

14. Ostacolo L, Marra M, Ungaro F, et al. In vitro anticancer activity of docetaxel-loaded micelles based on poly(ethylene oxide)-poly(epsilon-caprolactone) block copolymers: Do nanocarrier properties have a role? *J Control Release*. 2010;148:255–263. Epub September 8, 2010.

15. Gaucher G, Marchessault RH, Leroux JC. Polyester-based micelles and nanoparticles for the parenteral delivery of taxanes. *J Control Release*. 2010;143:2–12.

16. Liu B, Yang M, Li R, et al. The antitumor effect of novel docetaxel-loaded thermosensitive micelles. *Eur J Pharm Biopharm*. 2008;69:527–534.

17. Xu Z, Chen L, Gu W, et al. The performance of docetaxel-loaded solid lipid nanoparticles targeted to hepatocellular carcinoma. *Biomaterials*. 2009;30:226–232. Epub October 11, 2008.

18. Liu D, Wang L, Liu Z, Zhang C, Zhang N. Preparation, characterization, and in vitro evaluation of docetaxel-loaded poly(lactic acid)-poly(ethylene glycol) nanoparticles for parenteral drug delivery. *J Biomed Nanotechnol*. 2010;6:675–682.

19. Sundaram S, Durairaj C, Kadam R, Kompella UB. Luteinizing hormone-releasing hormone receptor-targeted deslorelin–docetaxel conjugate enhances efficacy of docetaxel in prostate cancer therapy. *Mol Cancer Ther*. 2009;8:1655–1665. Epub June 9, 2009.

20. Fite A, Goua M, Wahle KW, Schofield AC, Hutcheon AW, Heys SD. Potentiation of the anti-tumour effect of docetaxel by conjugated linoleic acids (CLAs) in breast cancer cells in vitro. *Prostaglandins Leukot Essent Fatty Acids*. 2007;77:87–96.

21. Esmaeili, F, Dinarvand, R, Ghahremani MH, et al. Docetaxel–albumin conjugates: preparation, in vitro evaluation and biodistribution studies. *J Pharm Sci*. 2009;98:2718–2730.

22. Lee E, Kim H, Lee IH, Jon S. In vivo antitumor effects of chitosan-conjugated docetaxel after oral administration. *J Control Release*. 2009;140:79–85.

23. Etrych T, Sírová M, Starovoytova L, Ríhová B, Ulbrich K. HPMA copolymer conjugates of paclitaxel and docetaxel with pH-controlled drug release. *Mol Pharm*. 2010;7:1015–1026.

24. Branco MC, Schneider JP. Self-assembling materials for therapeutic delivery. *Acta Biomater*. 2009;5:817–831.

25. Van S, Das SK, Wang X, et al. Synthesis, characterization, and biological evaluation of poly(L-γ-glutamyl-glutamine)-paclitaxel nanoconjugate. *Int J Nanomedicine*. 2010;5:825–837.

26. Wang X, Zhao G, Van S, et al. Pharmacokinetics and tissue distribution of PGG–PTX, a novel macromolecular formulation of paclitaxel, in nu/nu mice bearing NCI-460 lung cancer xenografts. *Cancer Chemother Pharmacol*. 2010;65:515–526.

27. Feng Z, Zhao G, Yu L, Gough D, Howell SB. Preclinical efficacy studies of a novel nanoparticle-based formulation of paclitaxel that outperforms Abraxane. *Cancer Chemother Pharmacol*. 2010;65:923–930. Epub August 15, 2009.

28. Yessine MA, Lafleur M, Meier C, Petereit HU, Leroux JC. Characterization of the membrane-destabilizing properties of different pH-sensitive methacrylic acid copolymers. *Biochim Biophys Acta*. 2003; 1613:28–38.

29. Maeda H, Wu J, Sawa T, Matsumura Y, Hori K. Tumor vascular permeability and the EPR effect in macromolecular therapeutics: a review. *J Control Release*. 2000;29:1723.

30. Fox ME, Szoka FC, Fréchet JM. Soluble polymer carriers for the treatment of cancer: the importance of molecular architecture. *Acc Chem Res*. 2009;42:1141–1151.

31. Duncan R. The dawning era of polymer therapeutics. *Nat Rev Drug Discov*. 2003;2:347–360.

32. Haag R, Kratz F. Polymer therapeutics: concepts and applications. *Angew Chem Int Ed*. 2006;45:1198–1215.

33. O'Brien MER, Socinski MA, Popovich AY, et al. Randomized phase iii trial comparing sing-agent paclitaxel Poliglumex (CT-2103, PPX) with single-agent gemcitabine or vinorelbine for the treatment of PS 2 patients with chemotherapy-naïve advanced non-small cell lung cancer. *J Thorac Oncol*. 2008;3:728–734.

34. Paz-Ares L, Ross H, O'Brien M, et al. Phase III trial comparing paclitaxel poliglumex vs docetaxel in the second-line treatment of non-small-cell lung cancer. *Br J Cancer*. 2008;98:1608–1613.

35. Langer CJ, O'Byrne KJ, Socinski MA, et al. Phase III trial comparing paclitaxel poliglumex (CT-2103, PPX) in combination with carboplatin versus standard paclitaxel and carboplatin in the treatment of PS 2 patients with chemotherapy-naïve advanced non-small cell lung cancer. *J Thorac Oncol*. 2008;3:623–630.

36. Yang D, Van S, Liu J, et al. Physicochemical properties and biocompatibility of polymer–paclitaxel conjugate for cancer treatment. *Int J Nanomedicine*. 2011;6:2557–2566. Epub October 21, 2011.

37. Yang D, Van S, Jiang X, Yu L. Novel free paclitaxel-loaded poly(L-γ-glutamylglutamine)-paclitaxel nanoparticles. *Int J Nanomedicine*. 2011;6:85–91.

38. Kwon S, Park JH, Chung H, Kwon IC, Jeong SY, Kim IS. Physico-chemical characteristics of self-assembled nanoparticles based on glycol chitosan bearing 5-cholanic acid. *Langmuir*. 2003;19:10188–10193.